Optical properties of $GaAs_{1-x}N_x$ on GaAs

W. K. Hung, M. Y. Chern, and Y. F. Chen
Department of Physics, National Taiwan University, Taipei, Taiwan, Republic of China

Z. L. Yang and Y. S. Huang
Department of Electronic Engineering, National Taiwan Institute of Technology, Taipei, Taiwan, Republic of China

(Received 12 June 2000)

The optical properties of $GaAs_{1-x}N_x$ with x up to 2.5% grown by metalorganic chemical vapor deposition on GaAs(001) substrates are reported. Fundamental band gaps are obtained by photoreflectance measurements. Room-temperature pseudodielectric functions obtained by spectroscopic ellipsometry in the range from 2.7 to 5.2 eV are modeled with a three-phase structure that accounts for the $GaAs_{1-x}N_x$ layer, native oxide, and ambient. We employ Adachi's critical-point composite model for the parametrization of $GaAs_{1-x}N_x$, and the compositional dependence of critical-point energies is obtained. While the energy of E_0 decreases with x, those of E_1 and $E_1+\Delta_1$ increase with x. This fact, somewhat anomalous compared with conventional III-V alloys, indicates that the lowest-lying conduction bands along $\langle 111 \rangle$ directions may be perturbed by the incorporated nitrogen.

I. INTRODUCTION

The incorporation of nitrogen atoms into III-V semiconductor hosts leads to a remarkable band-gap reduction, which makes such alloys of technological interest for long-wavelength optoelectronic devices[1,2] and multijunction high-efficiency solar cells.[3] In particular, a reduction of the band gap more than 0.1 eV per atomic percent of N content was observed in $GaAs_{1-x}N_x$ for $x<1.5\%$.[4] In contrast to conventional III-V semiconductor alloys, a composition-dependent bowing parameter of the order of 10–20 eV has to be introduced to describe the band-gap reduction.[5–7] It was shown experimentally and theoretically that the repulsing interaction between nitrogen-related state in the conduction band and the conduction-band edge is responsible for the large band-gap reduction.[8–11] Such a nitrogen-related state was observed in the electroreflectance spectra.[9] More recently, an unusual composition dependence of the conduction-band effective mass as a result of the formation of a nitrogen-related impurity band was also observed.[12] Furthermore, a strong composition dependence and bowing of the shear deformation potential of $GaAs_{1-x}N_x$ were found, which implies that not only the conduction-band but also the valence-band edge states are perturbed by the incorporated nitrogen.[13] These research studies indicate that the irregular electronic properties of $GaAs_{1-x}N_x$ near the band edge can be better understood by viewing nitrogen atoms as heavily doped isoelectronic impurities in GaAs, as contrasted with viewing $GaAs_{1-x}N_x$ as a dilute alloy.[13] Obviously, a more detailed study of the band structure of $GaAs_{1-x}N_x$ systems is required.

Due to the difficulty in preparing high-quality $GaAs_{1-x}N_x$ samples, optical studies including photoluminescence,[4,14] electroreflectance,[9,15] photoreflectance[8] (PR), photoconductivity,[16] and spectroscopic ellipsometry[17] (SE) measurements on this material were limited to $x<5\%$, while the optical transmission spectra[5] were measured up to $x\sim 15\%$. All the studies were limited to the fundamental gap region. On the other hand, the optical response properties of $GaAs_{1-x}N_x$ at energies greater than those of the fundamental band gap E_0 are of particular interest. This is because the structures in the optical spectra can be assigned to direct electronic transitions at specific regions of the Brillouin zone (BZ) and can therefore be related to the band structure of such systems.[18]

SE is a powerful technique that gives information on dielectric functions and band-structure critical points (CP's). In the present work, SE measurements of $GaAs_{1-x}N_x$ with x up to 2.5% were performed at room temperature. The data were analyzed for photon energies between 2.7 and 5.2 eV and the CP energies were identified by parametrizing the $GaAs_{1-x}N_x$ dielectric functions with Adachi's critical-point composite model.[19,20] The E_1 and $E_1+\Delta_1$ transition energies show a clear tendency to increase with increasing nitrogen content x, contrary to the case of the fundamental transition E_0, which decreases with x. This observation, although it seems to be ''anomalous'' as compared with the other zinc-blende semiconductor alloys (their E_1 and E_0 have the same trends with x), is probably consistent with the existence of nitrogen-induced states (or perturbations) above the conduction-band edge.

II. SAMPLE PREPARATION

The $GaAs_{1-x}N_x$ epitaxial layers with $x=0.20\%$, 0.56%, 1.20%, and 2.50% (in atomic percentage) were deposited on unintentionally doped GaAs buffers (~ 0.1 μm thick) on Si-doped GaAs(001) substrates by metalorganic chemical vapor deposition in a low-pressure (150 Torr) close-spaced vertical reactor. The reagents were triethylgallium, arsine, and dimethylhydrazine. Hydrogen was used as the carrier gas. The growth temperature was 550 °C. Samples were examined with a high-resolution x-ray diffractometer using the Cu $K\alpha_1$ line. Figure 1 shows the (004) x-ray spectra for two of the samples grown. Nitrogen compositions were determined by assuming the validity of Vegard's law and no strain relax-

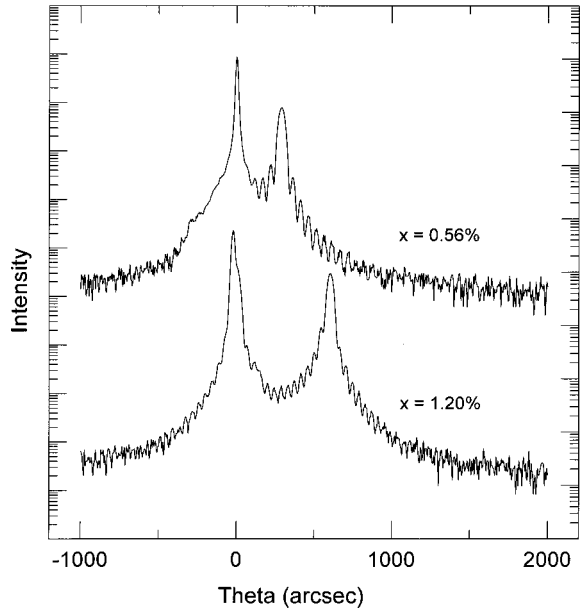

FIG. 1. High-resolution (004) x-ray diffraction spectra of $GaAs_{1-x}N_x$ grown on (001) GaAs substrates for $x=0.56\%$ and 1.20%.

ation. The latter assumption was verified by evaluation of the in-plane lattice constant obtained from the asymmetric {511} x-ray rocking curves. The lattice constants of GaAs and *c*-GaN used are 5.654 and 4.506 Å, respectively. The Poisson ratios are taken to be 0.310 and 0.366 for GaAs and *c*-GaN, respectively. The clear Pendellösung fringes shown in Fig. 1 indicate high crystalline quality and uniformity of the films and smooth interfaces between GaAs and $GaAs_{1-x}N_x$. The thickness of the films ranges from 380 to 480 nm, as determined from the separations of these fringes.

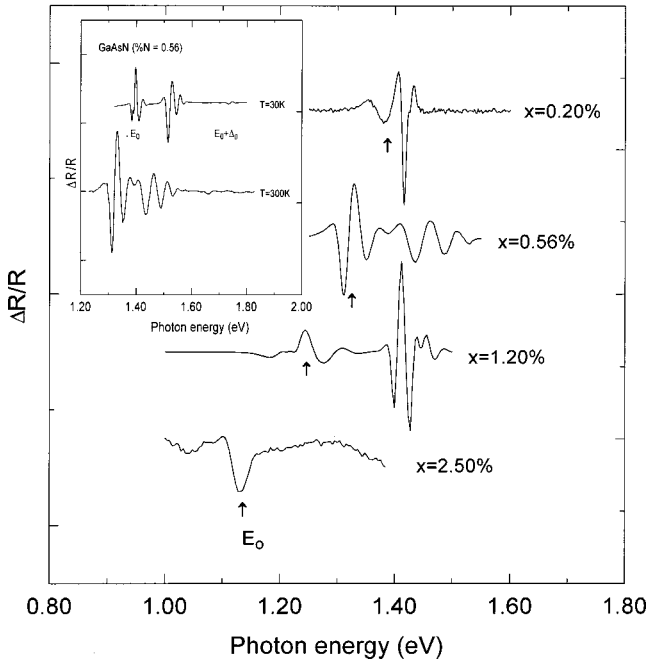

FIG. 2. Room-temperature PR spectra for $GaAs_{1-x}N_x$ samples. The band-gap transition E_0 of $GaAs_{1-x}N_x$ clearly shifts to lower energy as more nitrogen is added. The high-energy features correspond to the band-gap transition of GaAs substrates. The inset shows the PR spectrum (measured at 30 and 300 K) for the sample with $x=0.56\%$, which the transition $E_0+\Delta_0$ can be clearly seen.

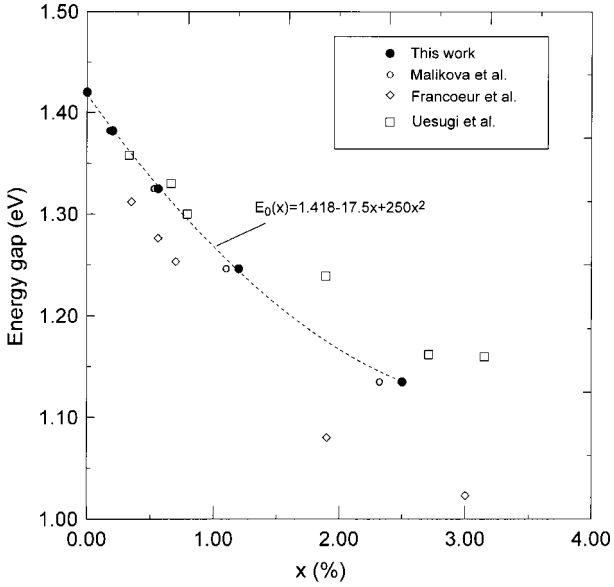

FIG. 3. Composition dependence of the room-temperature band-gap energy E_0 of $GaAs_{1-x}N_x$. The data from this work are shown as closed circles. Also shown are the experimental data taken from Refs. 6 (open squares), 14 (open diamonds), and 15 (open circles). The dashed line represents the best fit for our data.

III. PHOTOREFLECTANCE MEASUREMENTS

In order to obtain the energy gap E_0, room-temperature PR measurements were performed at near-normal incidence with an energy step of 2 meV. The experimental apparatus operated with a 150-W tungsten-halogen lamp as a probe source. The excitation source was provided by a 5-mW He-Ne laser mechanically chopped at a frequency of 200 Hz. The resulting spectra for all the samples are shown in Fig. 2. The transition energies are determined by fitting the spectra to the Aspnes third-derivative functional form[21] $\Delta R/R = \mathrm{Re}\{Ce^{i\theta}/(E-E_0+i\Gamma)^{5/2}\}$. Figure 3 shows E_0 as a function of nitrogen content *x*. As expected, E_0 redshifts with increasing *x*. Several data obtained by other authors are also shown for comparison. Our results agree well with those obtained by contactless electroreflectance measurements.[15]

The $E_0+\Delta_0$ feature corresponding to the transition from the split-off valence band was also observed for the sample with $x=0.56\%$, as is shown in the inset of Fig. 2. The obtained value of Δ_0 is 340 meV. Such a weak transition was not observed for the other samples possibly due to the film quality or the masking by the strong features from the GaAs substrate. Perkins *et al.*[9] performed electroreflectance measurements on a series of thick (2-μm) $GaAs_{1-x}N_x$ films and found that Δ_0 is nearly independent of the nitrogen composition for $x<2.8\%$.

IV. SPECTROSCOPIC ELLIPSOMETRY MEASUREMENTS

SE measurements on the samples were performed at room temperature using an automatic spectroscopic ellipsometer Sopra GESP5. The system uses a 75-W xenon lamp, a rotat-

ing polarizer, an autotracking analyzer, a double monochromator, and a single-photon-counting photomultiplier detector. Data were collected in the 1.4–5.2-eV photon energy region with the energy interval of 5 meV, at an incident angle of $\Phi = 75°$.

Ellipsometry determines the complex reflectance ratio ρ defined in terms of the standard parameters Ψ and Δ via

$$\rho = \frac{r_p}{r_s} = (\tan\Psi) e^{i\Delta}, \tag{1}$$

where r_p and r_s are the reflection coefficients for light polarized parallel (p) and perpendicular (s) to the plane of incidence, respectively. The pseudodielectric function $\langle\epsilon\rangle$, which is a common representation of the ellipsometric data Ψ and Δ, is obtained by treating the sample as a bulk (two-phase model):[22]

$$\langle\epsilon\rangle = \sin^2\Phi + (\sin^2\Phi)(\tan^2\Phi)\frac{(1-\rho)^2}{(1+\rho)^2} = \langle\epsilon_1\rangle + i\langle\epsilon_2\rangle. \tag{2}$$

The ellipsometric parameters depend on the photon energy, the sample layer structure, the material dielectric function of each layer, and the incident angle. A model calculation is needed for sample analysis. Instead of the apparent four-phase model (air–native oxide–$GaAs_{1-x}N_x$–GaAs), we limited our analysis to the energy region between 2.7 and 5.2 eV and treated our sample as a three-phase structure (air–native oxide–$GaAs_{1-x}N_x$). This is justified by the fact that the penetration depth ($<$550 Å) in this region is far less than the film thickness ($\sim$4000 Å) and the fact that the CP's such as E_1, $E_1+\Delta_1$, E_0', and E_2 are well included in this region. We do this for two reasons. First, our measurements did not cover the region below the band gap, where the interference effects (oscillating structures in the spectrum) would allow accurate determination of the film thickness. Second, the errors caused by the correlations between the parameters of the model dielectric function (MDF) and the thickness of $GaAs_{1-x}N_x$ layer can be avoided.

We employ Adachi's critical-point composite model for parametrization of the $GaAs_{1-x}N_x$ dielectric functions. Adachi's MDF is based on the one-electron interband-transition approach and includes terms for the E_0, $E_0+\Delta_0$, E_1, $E_1+\Delta_1$ transitions and phenomenological terms that describe contributions from high-lying transitions. In the following, we summarize the MDF for each CP. The detailed descriptions can be found in the literature.[19,20]

(A) E_0 and $E_0+\Delta_0$ transitions occur in the center of the BZ and are of the three-dimensional M_0 CP's:

$$\epsilon^{(0)}(E) = \sum_{j=0,s} A_j E_j^{-1.5}\{\chi_j^{-2}[2-(1+\chi_j)^{0.5}-(1-\chi_j)^{0.5}]\}, \tag{3}$$

with $\chi_j = (E+i\Gamma_j)/E_j$ ($j=0$ and s for E_0 and $E_0+\Delta_0$, respectively). A_j and Γ_j are, respectively, the strength and broadening parameter for each CP structure.

(B) The E_1 and $E_1+\Delta_1$ transitions for the III-V zinc-blende semiconductors take place along the $\langle 111\rangle$ directions of the BZ and are of the two-dimensional M_0 type:

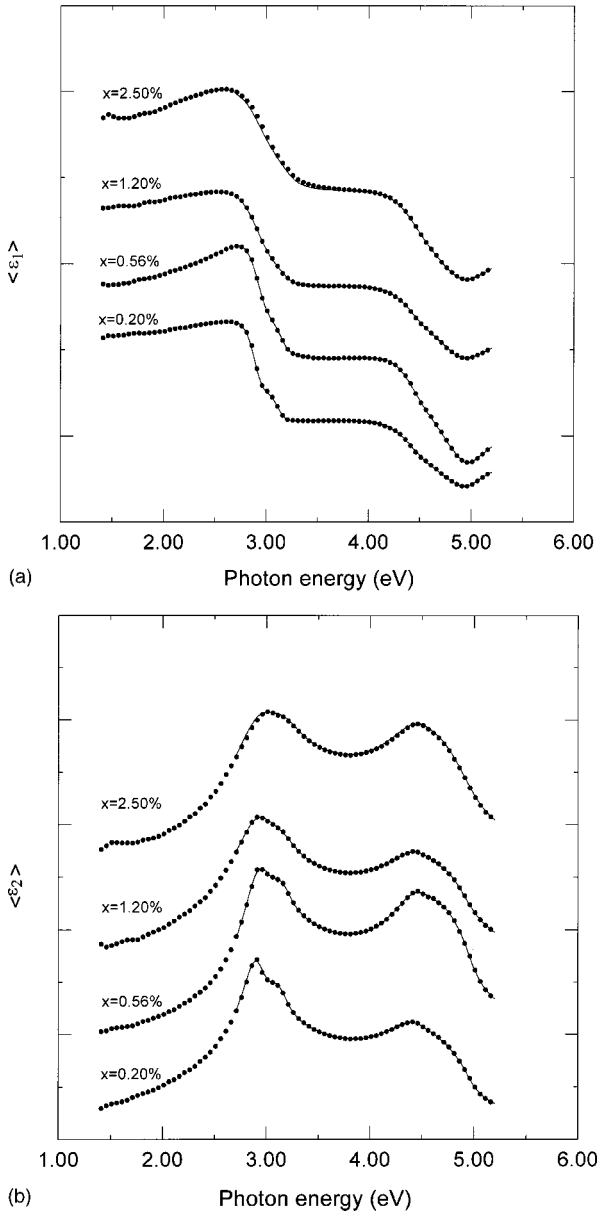

FIG. 4. (a) Real and (b) imaginary parts of pseudodielectric function $\langle\epsilon\rangle$ for $GaAs_{1-x}N_x$. The solid lines correspond to the best fit of the experimental data (represented by circles) to the three-phase model and the MDF parameters described in the text. Graphs are shifted for convenience.

$$\epsilon^{(1)}(E) = -\sum_{j=1,1s} B_j \chi_j^{-2}\ln(1-\chi_j^2), \tag{4}$$

with $\chi_j = (E+i\Gamma_j)/E_j$ ($j=1$ and $1s$ for E_1 and $E_1+\Delta_1$, respectively). B_j and Γ_j are, respectively, the strength and broadening parameter for each CP.

The contribution of the Wannier-type two-dimensional excitons to $\epsilon(E)$ can be written, with Lorentzian line shape, as

$$\epsilon^{(1x)}(E) = \sum_{n=1}^{\infty}\frac{1}{(2n-1)^3}\left(\frac{B_{1x}}{E_1-E-i\Gamma_1} + \frac{B_{2x}}{E_1+\Delta_1-E-i\Gamma_{1s}}\right), \tag{5}$$

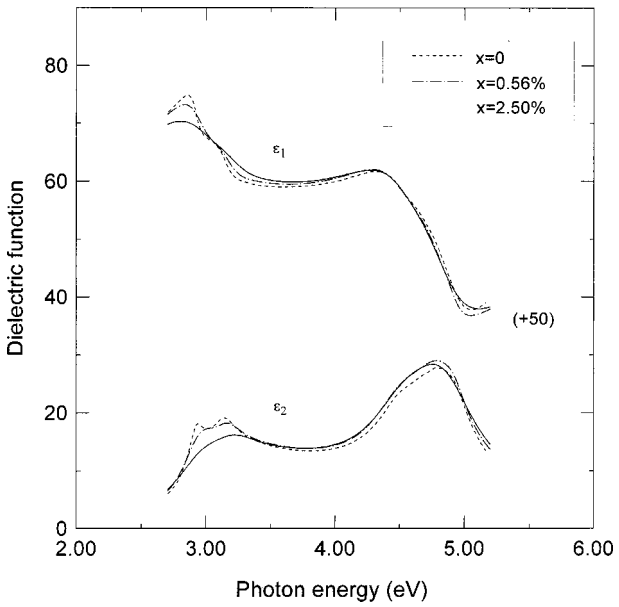

FIG. 5. Dielectric function $\epsilon=\epsilon_1+i\epsilon_2$ of $GaAs_{1-x}N_x$ extracted from the SE data using Adachi's critical-point composite model.

where B_{1x} (B_{2x}) is the strength parameter of the E_1 ($E_1+\Delta_1$) exciton.

(C) The pronounced structures in the spectrum in the region higher than E_1 are labeled E_0' and E_2 [$E_2(X)$ and $E_2(\Sigma)$, etc.]. They do not correspond to a single, well-defined CP and are characterized by three damped harmonic oscillations with energy E_j, strength parameter C_{E_j}, and damping constant Γ_{E_j}:

$$\epsilon^{(2)}(E)=\epsilon_\infty+\sum_{j=1}^{3}\frac{C_{E_i}E_j^2}{E_j^2-E^2-iE\Gamma_{E_i}}, \tag{6}$$

where ϵ_∞ is a constant included to account for the contribution of higher-lying transitions.

The complete model for the dielectric function is then obtained by summing over all these contributions:

$$\epsilon(E)=\epsilon^{(0)}(E)+\epsilon^{(1)}(E)+\epsilon^{(1x)}(E)+\epsilon^{(2)}(E). \tag{7}$$

To determine the unknown parameters (MDF parameters and oxide thickness), the Levenberg-Marquardt regression algorithm[23] was used to minimize the unbiased merit function

$$\chi^2=\sum_{i-1}^{N}[(\langle\epsilon_1\rangle_i^{\text{calc}}-\langle\epsilon_1\rangle_i^{\text{expt}})^2+(\langle\epsilon_2\rangle_i^{\text{calc}}-\langle\epsilon_2\rangle_i^{\text{expt}})^2], \tag{8}$$

where i indicates data sets ($\langle\epsilon_1\rangle$,$\langle\epsilon_2\rangle$) at photon energy E_i. $\langle\epsilon\rangle^{\text{expt}}$ represents the measured pseudodielectric function and $\langle\epsilon\rangle^{\text{calc}}$ represents the calculated pseudodielectric function from the three-phase model and the MDF. The CP energies E_0 and $E_0+\Delta_0$ were not treated as adjustable (unknown) parameters of the fit. The values of E_0 were determined from PR measurements, as shown above. The spin-orbit splitting Δ_0 was assumed to be a constant value 0.34 eV, as described in Sec. III. We assumed the optical constants of the $GaAs_{1-x}N_x$ native oxide to be the same as those of the GaAs, which can be found in the literature.[24] This is reasonable due to the very small amount of nitrogen content. The oxide thickness obtained for our samples with $x=0.20\%$, 0.56%, 1.20%, and 2.50% is 6.7, 4.0, 5.4, and 4.7 nm, respectively.

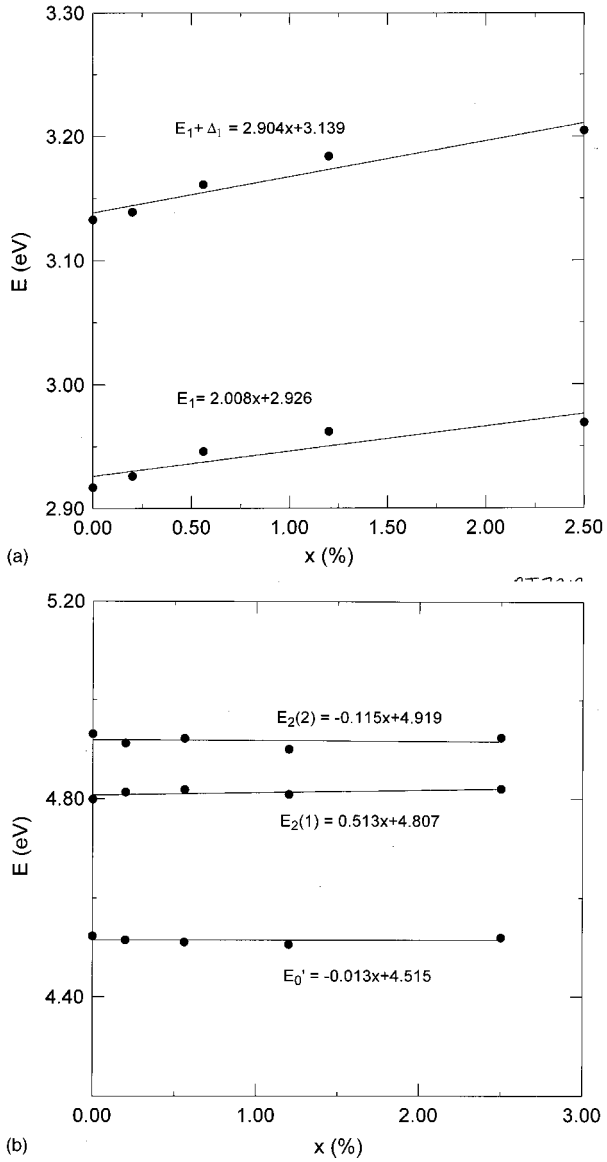

FIG. 6. Dependence of the $GaAs_{1-x}N_x$ CP energies on composition x. (a) for E_1 and $E_1+\Delta_1$ and (b) higher transitions labeled by E_0', $E_2(1)$, and $E_2(2)$. The solid lines represent the best fit of our data to linear functions.

Figure 4 shows real (a) and imaginary (b) parts of the pseudodielectric function $\langle\epsilon\rangle$ obtained from the four samples investigated here. The graphs are shifted for convenience. The symbols refer to the experimental data and the solid lines represent the best-fit calculation (in the range 2.7–5.2 eV). It can be seen that the best-fit curves match the experimental data very well.

The extracted $GaAs_{1-x}N_x$ dielectric functions are shown in Fig. 5. For clarity we only show the spectra for $x=0.56\%$ and 2.50%. The structures due to the E_1 and $E_1+\Delta_1$ transitions (around $E\sim3$ eV) shift toward higher-energy side with increasing x, but become broader and reduce in strength. It is noticeable, compared to conventional

III-V semiconductor alloys, that such a small amount of incorporated nitrogen can result in so large changes. One can expect that fairly large amounts of defects or compositional disorders may exist in the $GaAs_{1-x}N_x$ alloys due to the large difference in atomic size and electronegativity between As and N. Such disorders will cause a finite lifetime of the band states and their energy redistribution. This may partly account for the broadening of the E_1 and $E_1+\Delta_1$ structures. However, another possibility exists that the broadening may also be the consequence of some kind of perturbation on the band structure resulting from the N doping, as discussed below. On the other hand, the structures due to the E_0' and E_2 CP's do not show a clear trend with x compared with E_1 and $E_1+\Delta_1$.

The obtained CP energies as a function of x are plotted in Fig. 6. While the energies of E_0', $E_2(1)$, and $E_2(2)$ remain nearly unchanged, the energies of E_1 and $E_1+\Delta_1$ increase with increasing N composition, in contrast to the case of E_0 and $E_0+\Delta_0$. This behavior is somewhat ''anomalous'' when compared with other zinc-blende semiconductor alloy systems. One exception is the $Cd_{1-x}Mn_xTe$ alloys,[25] in which the energies of E_0 CP's increase with x while those of E_1 and $E_1+\Delta_1$ decrease slightly. This anomaly may be explained as due to a repulsion of the upper valence bands along $\langle 111\rangle$ directions by the occupied spin-up Mn $3d$ states. In the case of $GaAs_{1-x}N_x$, it is known that a single nitrogen in GaAs induces a resonant state E_N about 0.2 eV above the conduction-band minimum.[26] The repulsion between this resonant N level and the GaAs band-edge state (the two-level model) was proposed to explain the band-gap reduction and the observed N-related E_+ level above the conduction-band edge.[8,9] Since the energy separations between E_N and the conduction-band states along $\langle 111\rangle$ directions that participate in the E_1 and $E_1+\Delta_1$ transitions are not large (about 0.5–0.6 eV), it can be expected that the conduction-band states will be repelled to higher energies. Thus E_1 and $E_1+\Delta_1$ energies increase as nitrogen atoms are introduced into GaAs. Our result therefore implies the existence of the repulsion between nitrogen-related states and the conduction band in $GaAs_{1-x}N_x$. However, detailed theoretical and experimental investigations showed that the simple two-level repulsion model may be inadequate.[10,12,27] Instead, the mixing of the Γ and L conduction-band states, which results from the nitrogen-induced symmetry breaking, has been suggested recently as the origin of the observed E_+ level.[10,27] Such N-induced effects should also modify the band states along $\langle 111\rangle$ directions and thus affect the structures of dielectric function spectra around E_1 and $E_1+\Delta_1$ CP's. Further theoretical investigation is needed to clarify this point, which is beyond the scope of the present work.

Finally, it is worth pointing out that in order to interpret all the experimental results, the simple two-level model has to include the existence of the N pair bound states and how those levels evolve with increasing nitrogen composition.[12]

V. CONCLUSION

In conclusion, we have reported optical studies of the dielectric functions of $GaAs_{1-x}N_x$ layers on GaAs for x up to 2.50%. Fundamental band gaps determined from PR measurements show a very large bowing effect. The dielectric functions and the CP energies of the 2.7–5.2-eV region have been determined using room-temperature SE measurements. The E_1 and $E_1+\Delta_1$ transitions were found to shift toward higher photon energies with increasing x, while the E_0 (and $E_0+\Delta_0$) transition shows the opposite. This observation, which is anomalous compared with conventional alloy systems, may be a result of the N-induced modifications of the GaAs band structure. Our result calls for a further theoretical investigation of the band structure of $GaAs_{1-x}N_x$ material.

ACKNOWLEDGMENT

This work was partly supported by the National Science Council of the Republic of China.

[1] M. Kondow, K. Uomi, T. Kitatani, S. Watahiki, and Y. Yazawa, J. Cryst. Growth **164**, 175 (1996).
[2] G. S. Kinsey, D. W. Gotthold, A. L. Holmes Jr., B. G. Streetman, and J. C. Campbell, Appl. Phys. Lett. **76**, 2824 (2000).
[3] J. F. Geisz, D. J. Friedman, J. M. Olson, S. R. Kurtz, and B. M. Keyes, J. Cryst. Growth **195**, 401 (1998).
[4] M. Weyers, M. Sato, and H. Ando, Jpn. J. Appl. Phys., Part 2 **31**, L853 (1992).
[5] W. G. Bi and C. W. Tu, Appl. Phys. Lett. **70**, 1608 (1997).
[6] K. Uesugi and I. Suemune, Jpn. J. Appl. Phys., Part 2 **36**, L1572 (1997).
[7] S. H. Wei and A. Zunger, Phys. Rev. Lett. **76**, 664 (1996).
[8] W. Shan, W. Walukiewicz, J. W. Ager III, E. E. Haller, J. F. Geisz, D. J. Friedman, J. M. Olson, and S. R. Kurtz, Phys. Rev. Lett. **82**, 1221 (1999).
[9] J. D. Perkins, A. Mascarenhas, Y. Zhang, J. F. Geisz, D. J. Friedman, J. M. Olson, and S. R. Kurtz, Phys. Rev. Lett. **82**, 3312 (1999).
[10] T. Mattila, S.-H. Wei, and A. Zunger, Phys. Rev. B **60**, R11 245 (1999).
[11] A. Lindsay and E. P. O'Reilly, Solid State Commun. **112**, 443 (1999).
[12] Y. Zhang, A. Mascarenhas, H. P. Xin, and C. W. Tu, Phys. Rev. B **61**, 7479 (2000).
[13] Y. Zhang, A. Mascarenhas, H. P. Xin, and C. W. Tu, Phys. Rev. B **61**, 4433 (2000).
[14] S. Francoeur, G. Sivaraman, Y. Qiu, S. Nikishin, and H. Temkin, Appl. Phys. Lett. **72**, 1857 (1998).
[15] L. Malikova, F. H. Pollak, and R. Bhat, J. Electron. Mater. **27**, 484 (1998).
[16] W. K. Hung, M. Y. Chern, J. C. Fan, T. Y. Lin, and Y. F. Chen, Appl. Phys. Lett. **74**, 3951 (1999).
[17] J. Sik, M. Schubert, G. Leibiger, v. Gottschalch, G. Kirpal, and J. Humlíček, Appl. Phys. Lett. **76**, 2859 (2000).
[18] M. L. Cohen and J. R. Chelikowsky, *Electronic Structure and Optical Properties of Semiconductors* (Springer, Berlin, 1988).
[19] S. Adachi, T. Kimura, and N. Suzuki, J. Appl. Phys. **74**, 3435 (1993).
[20] S. Ozaki and S. Adachi, J. Appl. Phys. **78**, 3380 (1995).
[21] D. E. Aspnes, Surf. Sci. **37**, 418 (1973).

[22] R. M. A. Azzam and N. M. Bashara, *Ellipsometry and Polarized Light* (North-Holland, Amsterdam, 1977).
[23] W. H. Press, B. P. Flannery, S. A. Teukolsky, and W. T. Vetterling, *Numerical Recipes* (Cambridge University Press, Cambridge, 1988).
[24] G. E. Jellison Jr., Opt. Mater. **1**, 151 (1992).
[25] P. Lautenschlager, S. Logothetidis, L. Viňa, and M. Cardona, Phys. Rev. B **32**, 3811 (1985).
[26] D. J. Wolford, J. A. Bradley, K. Fry, and J. Thompson, in *Proceedings of the 17th International Conference on the Physics of Semiconductors*, edited by J. D. Chadi and W. A. Harrison (Springer, New York, 1984), p. 627.
[27] H. M. Cheong, Y. Zhang, A. Mascarenhas, and J. F. Geisz, Phys. Rev. B **61**, 13 687 (2000).